Supporting Information

Kandyba et al. 10.1073/pnas.1121312110

SI Materials and Methods

Histology. Tissues for immunofluorescence and H&E staining were embedded in Optimal Cutting Temperature compound (OCT) and frozen immediately on dry ice. Twelve-micrometer–thick cryosections were taken and kept at −20 °C until required for staining. For paraffin embedding, skin samples were fixed overnight in 4% (vol/vol) paraformaldehyde, and the following day were washed thoroughly in PBS. Samples were then dehydrated through an alcohol series before embedding in paraffin and sectioning. Paraffin sections were cleared in xylene and hydrated before staining.

Immunofluorescence and BrdU Labeling. Histology and immunofluorescence were performed as described. The following antibodies were used at the indicated dilutions: CD34 (rat, 1:50; eBioscience); BrdU (rat, 1:200; Abcam); P-cadherin (goat, 1:100; R&D Systems); Wnt7a (rabbit, 1:100; Sigma), Wnt7b (rabbit, 1:100; Abcam), Fzd10 (goat, 1:100; Santa Cruz), β-catenin (mouse, 1:50; Sigma), and Ki67 (rabbit, 1:300; Novocastra). Relevant FITC- or Texas Red-conjugated secondary antibodies (1:300; Sigma) were used for detection. Images were captured on an upright Zeiss fluorescent microscope and processed in Adobe photoshop. For pulse experiments, BrdU (Sigma-Aldrich) was administered by intraperitoneal injection at P59 or P62 mice (50 $\mu g \cdot g^{-1} \cdot d^{-1}$) for 3 h before analyses (1).

FACS Analysis. Purification of bulge hfSCs from adult mouse back skins was described previously (1). For FACS analysis and isolation of YFP+ hfSC populations, we used the following primary antibodies: anti-a6 integrin (CD49f) conjugated to PE (1:200; BD Pharminogen) and anti-CD34 coupled to Alexafluor 700 (1:50; eBioscience). Cells were collected in RNAprotect Cell Reagent (Qiagen) for later RNA isolation or media for cell culture experiments. For hair germ (HG) FACS analysis, at P59 and P62 primary antibody P-cadherin (Pcad) (1:100; R&D Systems) was used conjugated to Allophycocyanin (APC). At P59, the proliferation status of the YFP+ hfSC populations was determined in control after RU486 treatment (Con^{RU})and RU486 inducible conditional knockout (cKO^{RU}) mice after receiving a 3-h BrdU pulse. FACS analysis was performed (as described in *Materials and Methods*). Briefly, YFP+ Con^{RU} and cKO^{RU} hfSC populations were collected and fixed for 10 min at 4 °C in 4% (vol/vol) paraformaldehyde. Then, in the second step, collected YFP+ Con^{RU} and cKO^{RU} hfSCs were washed in PBS and stained with the APC BrdU Flow Kit (BD Pharminogen) according to the manufacturer's instructions to assay for BrdU incorporation.

For FACS analysis of Phospho-Smad1,5,8 (P-Smad1,5,8) expression in control and K15-GFP+/dTg hfSCs after oral Doxy administration at P25, control and K15-GFP+/dTg mice were killed and the dorsal skin prepared for FACS sorting in the presence of phosphatase inhibitors. To help preserve the P-Smad status in the hfSC population, K15-GFP+ cells were collected and fixed directly in 4% (vol/vol) paraformaldehyde at 4 °C for 10 min. Fixed cells were then incubated with P-Smad1,5,8 antibody (rabbit, 1:50; Cell Signaling) for 30 min on ice and then washed thoroughly before incubating with secondary anti-rabbit–Alexa 647 (1:100; Invitrogen) for 30 min in the dark on ice. Cells were then washed and resuspended for FACS analysis of P-Smad1,5,8 expression.

Cell Culture and Colony-Forming Assay. Cells collected from FACS analysis were plated directly onto mitomycin-treated 3T3 fibroblast feeder layers and left to attach overnight. The following day, cultures were carefully washed with PBS, and fresh media was added. For attachment and colony-forming assays, ∼100 cells (CON or KO) were seeded onto 10-cm mitomycin-treated 3T3 feeder layers and left to attach (∼9 h) after which the number of attached cells were counted in triplicate. The following day, cultures were washed in PBS, and the culture media was changed. YFP+ colony sizes were monitored and counted daily for 7 d when cell cultures were trypsinized and prepared for FACS analysis to quantify total YFP+ cell populations.

RNA Isolation, Semiquantitative RT-PCR, and qPCR. Total RNAs were purified from FACS-sorted hfSCs using a Qiagen RNeasy kit according to the manufacturer's instructions. Equal amounts of RNA were reverse-transcribed using the SuperScript III First-Strand Synthesis System (Invitrogen) according to the manufacturer's instructions. cDNAs were amplified by PCR, and 200 ng cDNA were then used in triplicate for each qPCR sample primer set with all primer sets designed to work under the same conditions. Real-time PCR amplification of particular genes of interest was performed using a Roche LightCycler 480, and the fold difference between samples and controls was calculated based on the 2-ΔΔCT method, normalized to Gapdh levels.

Growth Factor-Mediated Delivery Using Soaked Beads. Human recombinant Wnt7a was obtained from R&D Systems and reconstituted in 0.1% BSA according to the manufacturer's guidelines. Affi-gel blue gel beads (Bio-Rad) were washed three times in sterile PBS and then resuspended with recombinant protein [(vol/vol) in 0.1% BSA] at 4 °C for 1 h before injection. To test the effects of recombinant protein, the following concentration was used: 100 ng/20 μL Wnt7a (R&D Systems). For each protein examined (or PBS bead control), five daily s.c. injections were performed to the same skin region using a 26G syringe, introducing ∼100 beads/20 μL bead solution under the back skin from P54 to P59.

Chamber Graft in Vivo Reconstitution Assay. Separately, cultured YFP+ hfSCs from both cKO^{RU} and CON^{RU} (1 million cells at passage 4) were combined with freshly isolated dermal fractions from newborn mice (at a 1:1 ratio), and these epidermal and dermal cell suspensions were engrafted onto athymic mice (2). Mice were killed, and samples from the graft regions were taken for YFP+ expression and tissue analysis.

Microarray Analysis. Total RNAs from FACS cells were purified using a RNeasy Micro Kit (Qiagen) and quantified (Nanodrop). RNA 6000 Pico Assay (Agilent Technologies) was used to assess RNA quality. Amplification and labeling were performed on 50 ng to obtain biotinylated cRNA (Ovation RNA Amplification System; Nugen), and 3.75 μg ssDNA was used for fragmentation, labeling, and hybridization. Hybridization was performed at 45 °C for 18 h to mouse genome array MOE430A2.0 (Affymetrix). Processed chips were read by a GeneChip Scanner 3000 7G (Genomics Core Facility, Children's Hospital, Los Angeles).

The raw expression intensity data were imported into Partek Genomic Suite v6 (Partek Inc.). The data were preprocessed using the RMA algorithm with the default Partek setting. Following fold-change calculations, gene lists containing probe sets with twofold intensity changes in either direction were generated.

For overlap comparisons with previously published hair bulge and HG gene signatures (1, 3–5), the common Affymetrix probe sets were extracted from the BMP inhibition datasets after BMP inhibition, and the percentages of common genes in the signature

lists were calculated. Because we used the same mouse genome array (MOE430A2.0), the probe set IDs were used for comparison with hair bulge signature genes. Functional annotation of probe set lists was carried out using the Database for Annotation, Visualization and Integrated Discovery.

In Vivo hfSC ChIP Assay. In vivo ChIP was performed using cells directly FACS-sorted from *Bmpr1a* gain-of-function K15-GFP+/dTg mice at P21 (6) (with or without Doxy food from P18 to P21) in the presence of phosphatase inhibitors. Approximately 3×10^6 K15-GFP cells (bulge hfSCs) were isolated from both control and dTg samples and fixed in 1% (vol/vol) formaldehyde and then quenched with 0.125 M glycine. Cells were then snap-frozen and stored at −80 °C until required for further processing. Samples were prepared using a Qiagen EpiTect ChIP OneDay Kit according to the manufacturer's instructions. DNA was sheared by sonication to an average length of 500 bp (as measured by electrophoresis), and P-Smad1,5,8 (rabbit, 1:50; Cell Signaling) or control IgG (rabbit, 1:50; Sigma) was added to each sample to form immunocomplexes. Putative Smad-binding sites were identified with BioBase Promoter analysis software, and 5′ upstream ChIP primer sequences were designed (with the aid of Ensemble software) based on clustering of Smad-binding sites (primarily Smad1,5,8) with PCR performed using input or immunoprecipitated DNA and primers designed to amplify specific regions of the indicated promoters.

Promoter Analyses for SMAD-Binding Sites. Computer predictions (Biobase; BKL TRANSFAC promoter analyses software) of SMAD 1, 5, 8 binding sites within the promoter regions of each selected BMP-signaling target gene were used.

1. Blanpain C, Lowry WE, Geoghegan A, Polak L, Fuchs E (2004) Self-renewal, multipotency, and the existence of two cell populations within an epithelial stem cell niche. *Cell* 118(5):635–648.
2. Weinberg WC, et al. (1993) Reconstitution of hair follicle development in vivo: Determination of follicle formation, hair growth, and hair quality by dermal cells. *J Invest Dermatol* 100(3):229–236.
3. Tumbar T, et al. (2004) Defining the epithelial stem cell niche in skin. *Science* 303(5656): 359–363.
4. Lowry WE, et al. (2005) Defining the impact of beta-catenin/Tcf transactivation on epithelial stem cells. *Genes Dev* 19(13):1596–1611.
5. Greco V, et al. (2009) A two-step mechanism for stem cell activation during hair regeneration. *Cell Stem Cell* 4(2):155–169.
6. Kobielak K, Stokes N, de la Cruz J, Polak L, Fuchs E (2007) Loss of a quiescent niche but not follicle stem cells in the absence of bone morphogenetic protein signaling. *Proc Natl Acad Sci USA* 104(24):10063–10068.

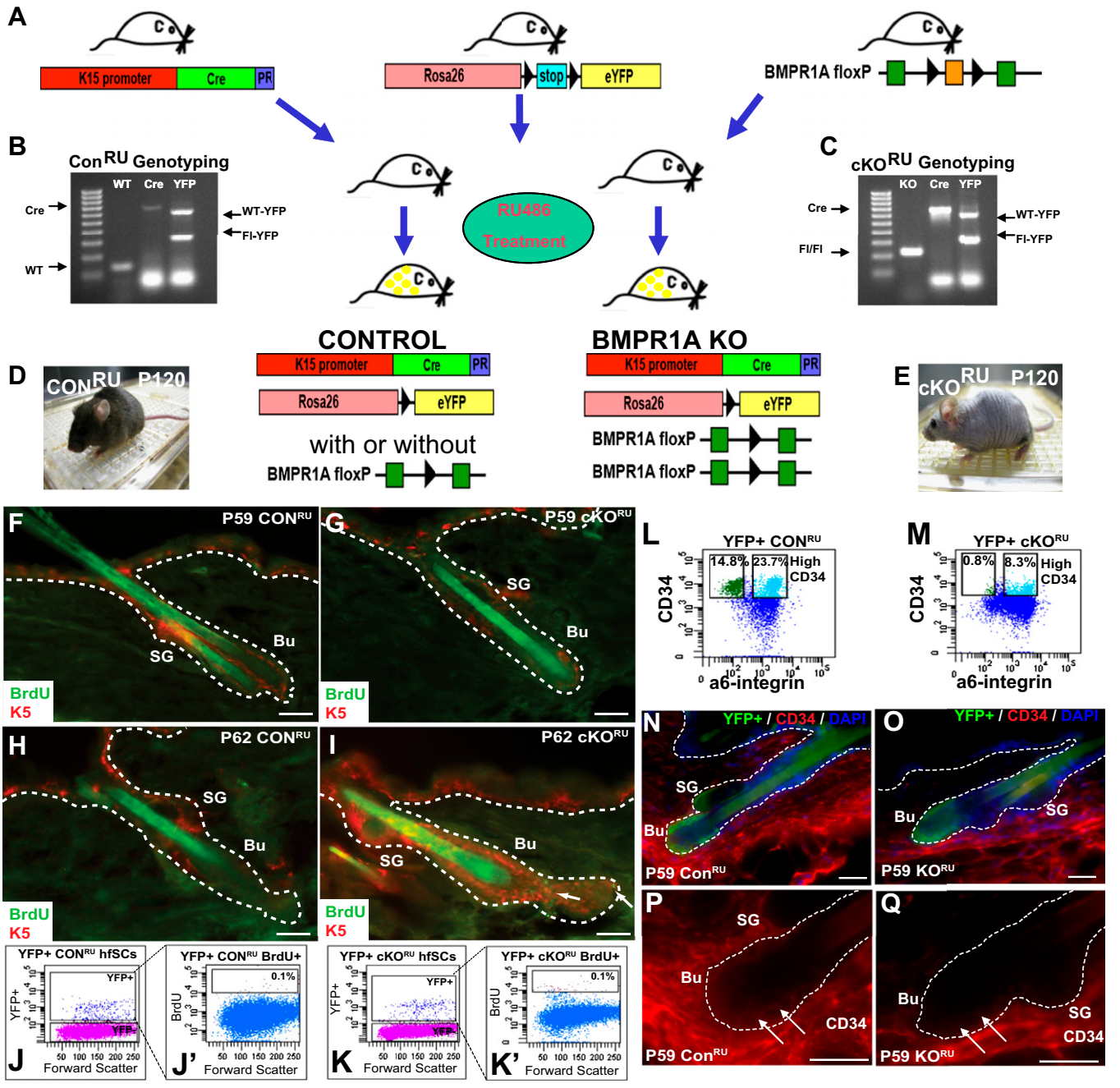

Fig. S1. Generation of conditional, inducible knockout mice to specifically label and inactivate BMP signaling in hfSCs. (*A*) Schematic depicting matings between three different lines of mice: K15-CrePR × *Bmpr1a* flox/flox (FL/FL) × Rosa26-Stop-YFP(FL/FL). (*B* and *C*) Genotyping of the offspring from these matings: Con^{RU} corresponding to K15CrePR/*Bmpr1a* WT/WT/YFP (Fl/WT) and cKO^{RU} indicates K15CrePR/*Bmpr1a* Fl/Fl/YFP (Fl/WT). (*D* and *E*) Phenotype of adult Con^{RU} and cKO^{RU} mice, respectively, after RU treatment where cKO^{RU} mice did not regrow hair at P120. (*G* and *F*) After a 3-h BrdU pulse, BrdU staining showed quiescence of both cKO^{RU} and CON^{RU} hfSCs at P59. (*I*) At P62, BrdU staining in cKO^{RU} follicles displayed precocious anagen activation with BrdU-labeled cells in the bulge and HG (arrows). (*H*) In contrast, CON^{RU} follicles were still in telogen with no BrdU staining. (*J*–*K*′) Comparable BrdU incorporation was observed at P59 in both Con^{RU} (*J* and *J*′) and cKO^{RU} (*K* and *K*′) in YFP+ hfSC populations by FACS analysis. (*M* and *L*) Upon BMP-signaling inactivation, although remaining in telogen morphologically, expression of the CD34 marker in cKO^{RU} hfSCs was considerably decreased compared with CON^{RU} YFP+ CD34 high fractions by FACS. (*N* and *P*) YFP+ population of bulge cells positive for CD34 staining in CON^{RU} (arrows). (*O* and *Q*) YFP+ cKO^{RU} bulge cells with decreased staining for CD34 (arrows). cKO^{RU}, conditional knockout after RU treatment; Con^{RU}, control; Cre-PR, recombinase conjugated with truncated progesterone receptor; floxP and FL, loxedP site; YFP, yellow fluorescent protein. (Scale bars: 50 μm.)

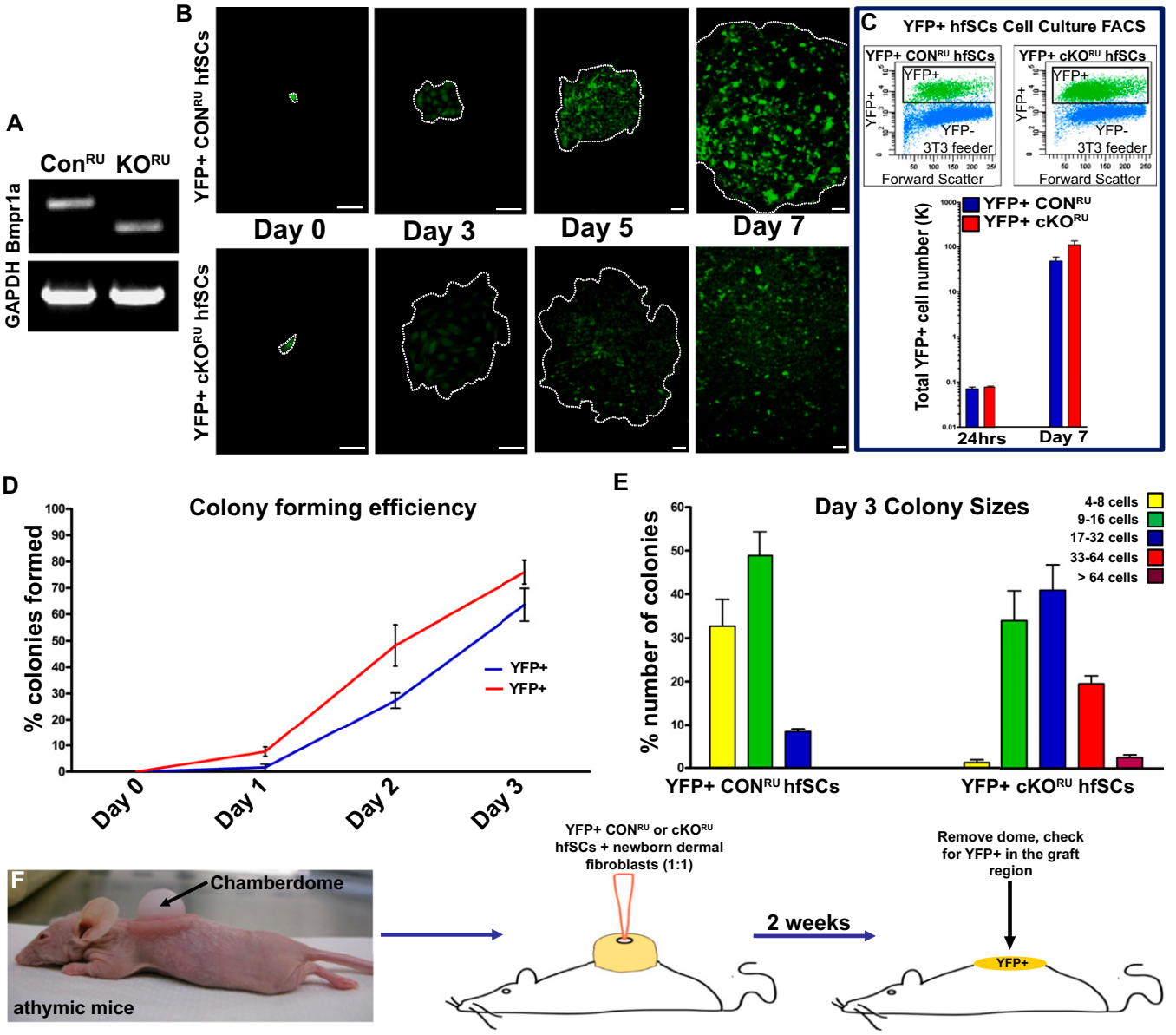

Fig. S2. hfSCs after BMP inhibition maintain stem cell characteristics in vitro. Chamber graft reconstitution assay. (*A*) YFP+ basal hfSC populations from both CON^{RU} and cKO^{RU} sorted positively for α6-integrin, and CD34 by FACS was used for microarray analysis; loxP high- recombination efficiency for exon 2 deletion in the cKO^{RU} hfSC population was confirmed by RT-PCR compared with CON^{RU} hfSC and GAPDH controls. (*B*) YFP+ CON^{RU} and cKO^{RU} hfSCs were isolated by FACS and grown as holoclones on mitomycin-treated 3T3 fibroblast feeder layers, resulting in the formation of YFP+ colonies. Both cKO^{RU} and CON^{RU} hfSCs formed regular, tightly packed YFP+ holoclone colonies; however, cKO^{RU} YFP+ hfSCs cells formed larger colonies as shown in days 3, 5, and 7. (*C*) Similar attachment rates were demonstrated after plating the same number of YFP+ sorted cells from CON^{RU} and cKO^{RU} HFs for 24 h. However, over a period of 7 d, cKO^{RU} hfSCs displayed a faster proliferation rate, and FACS analysis (*C*, *Upper* panels) showed a higher percentage of YFP+ cells in cKO^{RU} colonies compared with CON^{RU} colonies at day 7. (*D*) During the first 3 d, YFP+ cKO^{RU} hfSCs demonstrated slightly higher colony-forming efficiency than CON^{RU}. (*E*) YFP+ cells from cKO^{RU} hfSCs formed significantly larger colonies than CON^{RU} with a higher average cell number per colony. (*F*) Photo and schematic of chamber graft experiments to reconstitute skin in vivo. YFP+ cultured hfSCs from both cKO^{RU} and CON^{RU}. Approximately 1 million cells at passage 4 or 6 were mixed with freshly isolated dermal fibroblasts from newborn mice at P0 in a 1:1 ratio, and then mixtures of cells were engrafted onto athymic mice. After approximately 2 wk, domes were removed and skin was checked for YFP expression in grafted regions. (Scale bars: 50 μm.)

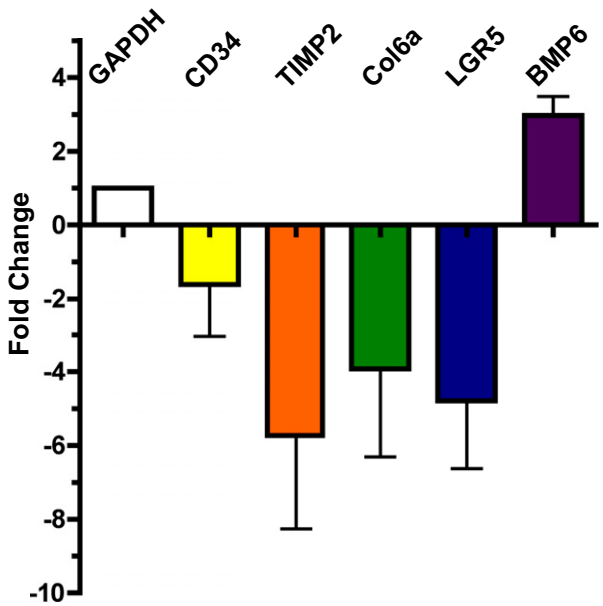

Fig. S3. Validation of randomly chosen genes changed in cKO^{RU} hfSCs. qPCR of randomly chosen genes changed in cKO^{RU} hfSCs confirmed microarray data using independent FACS-isolated biological samples.

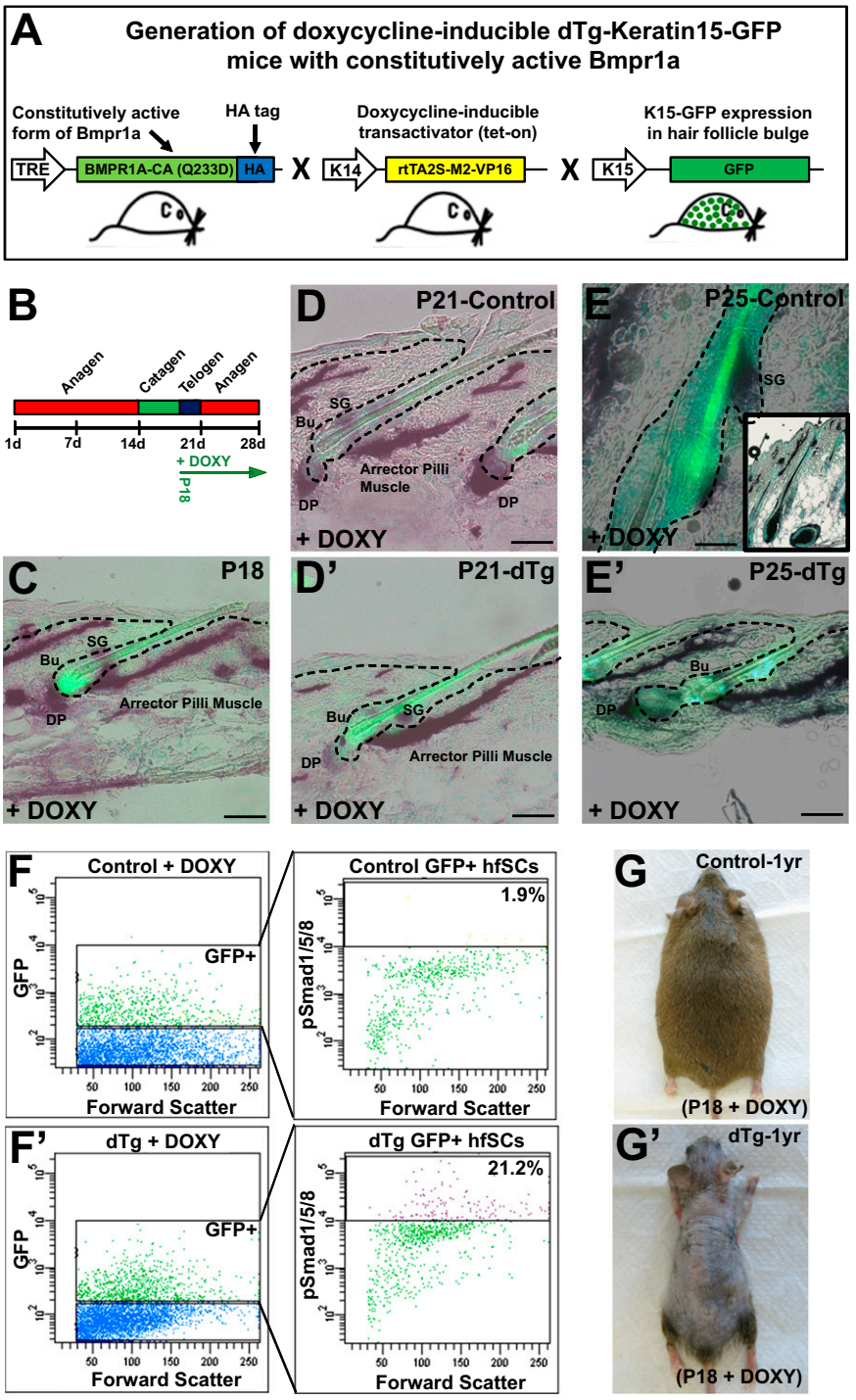

Fig. S4. Engineering of conditional dTg mice to specifically label and isolate hfSCs with activated BMP signaling in vivo. (*A*) Schematic depicting matings between three different lines of mice: dTg for the TRE-constitutively active BMP receptor 1A (a constitutively active form of *Bmpr1a*) with K14-rtTA (a Doxy-inducible transactivator) and K15-GFP mice to facilitate isolation of hfSCs in vivo after oral administration of Doxy and BMP-signaling activation. (*B*) Chart illustrating the temporal progression through the first postnatal hair cycle starting Doxy administration at P18. (*C–E′*) Alkaline phosphatase staining labeled morphological positions of dermal papilla and arrector pilli muscle relative to the bulge region (marked with K15-GFP expression) on skin sections at P18, P21, and P25. (*C–D′*) At P18 and P21, both control and K15-GFP+/dTg hair follicles remained morphologically in telogen. (*E* and *E′*) At P25, control hair follicles were at midanagen stage; in contrast, K15-GFP+/dTg hair remained morphologically in a prolonged telogen stage. (*F* and *F′*) In vivo, FACS-sorted K15-GFP–positive hfSCs demonstrated increased Phospho-Smad (P-Smad) levels in the K15-GFP+/dTg mice, compared with control hfSCs after oral administration of Doxy at P25. (*G′*) Long-term consequences of prolonged constitutive activation of BMP signaling in the hfSC population results in a progressive hair loss phenotype in K15-GFP+/dTg mice, whereas control mice on Doxy display no visible hair abnormalities (*G*). (Scale bars: 50 μm.)

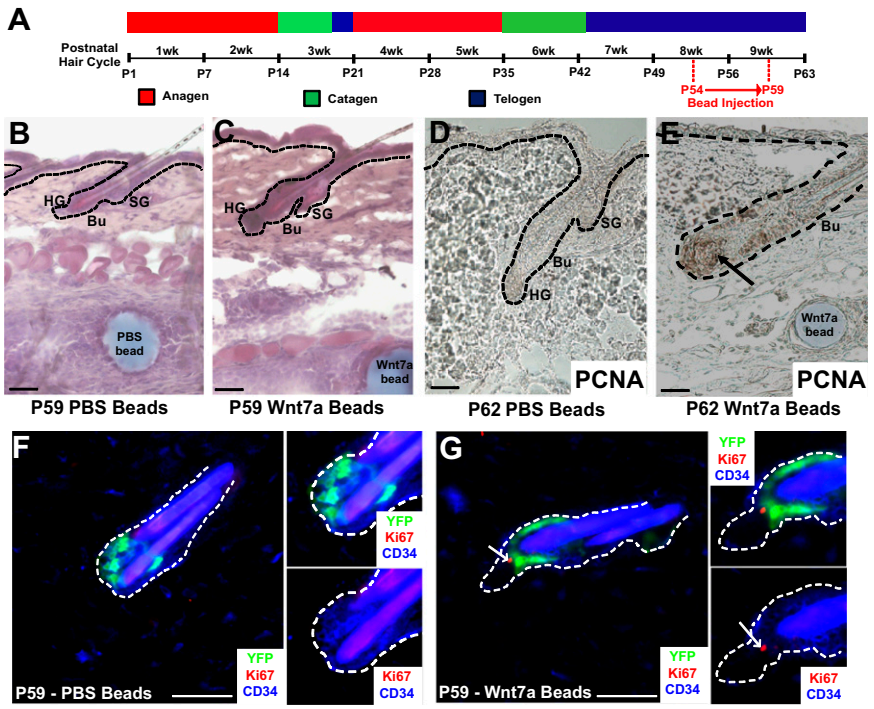

Fig. S5. Subcutaneous injection of Wnt7a recombinant protein induces a precocious telogen-to-anagen transition via canonical Wnt signaling. (*A*) Chart illustrating the 5 d of consecutive daily bead injections during the second postnatal telogen and the time points at which the samples were collected for analysis. (*C*) At P59, H&E staining revealed increased HG size of HFs in the direct vicinity of Wnt7a-coated beads. (*B*) In contrast, control HFs remained in telogen. (*E*) PCNA staining at P62 showed proliferation of HFs after ectopic Wnt7a injection. (*D*) In contrast, PCNA staining was not observed in control HFs that remained in telogen. (*G*) At P59, following s.c. Wnt7a injection, hair follicles in the vicinity of beads displayed triple-positive cells for Ki67 staining (red channel, arrow), CD34 (blue channel), and YFP (green channel) in the lower bulge region, whereas control HFs at the same time point remained in telogen without Ki67-positive cells (*F*). Note the higher magnification of the bulge and HG region in the *Insets* on the right in *F* and *G*. (Scale bars: 50 μm.)

	Up-regulated Telogen Bulge Hair Follicle Stem Cell Signature Genes	BMP as a Master Molecular Switch: Common Signature Genes Affected By BMP Signaling	Down-regulated Hair Germ Signature Genes
Cell Cycle	Cdkn2b, Has2, Hist2h3c2, Lgals1, Lgals7	Nbl1	Pmp22, Gas1, Sesn1
Signaling	Adamtsl4, Alcam, Angptl2, Aplp1, App, Arvcf, Aspn, Bdnf, Blnk, Boc, C1ql3, C1qdc2, C9, Cadm1, Ccl27, Crispld1, Cspg4, Ctgf, Ctsf, Ctsz, Cxcl14, Dab2, Dclk1, Ddit4l, Dmpk, Dusp14, Egfl6, Emb, Epdr1, Eps8, EphrinA5, Fbln1, Fbn2, FGF1, Frap1, Fst, Fstl1, Fzd7, Gdf10, Glrb, Gkap1, Gpc6, Grb14, Grik, Gsn, Hexa, Hexb, Hhip, Homer2, Hsd17b11, Igfbp5, Il11ra2, Il31ra, Mansc1, Mark1, Mfge8, Myoc, Nek3, Nenf, Nope, Nrcam, Nptx1, Odz2, Ophn1, Pi4k2b, Pik3r1, Pkd1, Pkd2, Plxna2, Plat, Ppap2b, Pqlc3, Pthlh, Ptn, Ptprk, Pvrl4, Rab15, Ramp1, Ramp3, Rhpn2, Scrg1, Scube2, Sdc2, Sdc3, Sectm1b, Sema3e, Sh3kbp1, Sh3rf1, Slit3, Smoc1, Smpdl3b, Sncg, Sulf2, Thsd1, Them4, Tirap, Tmem34, Tmem46, Tmem158, Tnfrsf11b, Trp53i13, Vwa1	BMP6, Dkk3, FGF18, Fzd2, Fzd3, Grem1, Lgr5, Ltbp2, Ltbp3, Ppap2a, Sfrp1	Fst, Fzd7 Ltbp4, Sema3e
Transcription Factors	Aplp2, Cbx6, Cebpd, Cited, Dlx5, Enc1, Foxc1, Foxp1, Hey1, Hopx, Hoxa9, Hoxb5, Hoxb6, Hoxc8, Hoxd8, Hoxd9, Hmga2, Grip1, ID4, Jundm2, Klhdc2, Klhl22, Lhx2, Lmo1, Lmo7, Lrrfip1, Mitf, Smad7, Sox9, Tceal1, Tcf7l2, Tcfap2b, TCF3, Tbx1	ID2, ID3, NFATc1	ID4, Lhx2, Nfib, Sox9, TCF3, Vdr
ECM / Cell Adhesion	Amot, Col1a1, Col1a2, Col9a3, Col3a1, Col4a2, Col5a2, Col6a2, Duoxa1, Macf1, Pfn2, Pkp2, TIMP2, S100a1, S100a4, S100a6, Sdcbp, Ssx2ip, St6galnac5, Ugdh, Zyx	CD34, Col6a1, Ecm1	Cdh13, Macf1, Pfn2, S100a6
Miscellaneous	Actn1, Aig1, Akr1c14, Ankrd24, Aldoc, Aktip, Ank, Appl2, Aqp3, Aqp5, Arid5A, Armcx2, Armcx3, Atp6v0e2, Atp8a2, Auh, BB146404, BC023055, Bcl2l11, Cald1, Calml3, Capn6, Cacna1c, Cbr4, Cdc42ep3, Chd6, Cmtm3, Cmtm8, Copz2, Creb3l4, Crip1, Cryab, Cyp2b10, Cyp2d22,Cyba, D0H4S114, D9Ertd280e, Dap, Dapk2, Degs1, Dleu2, Dlgap4, Dnaja4, Dmd, Dysf, Edg7, Edg8, Efcab4a, Elavl2, Emp3, Enah, Enpp1, Ephx1, Farp1, Fchsd1, Fermt2, Fermt3, Fhl1, Flnb, Ft1, Gabarapl1, Gdpd1, Gphn, Gpm6b, Gpr137b, Gnb1l, Hpgd, Hpcal1, Hpcal1, Hspa4l, Hspb8, Idh2, Ier3, Ift57, Ift81, Ints6, Iqsec1, Itm2a, Kcnk2, Kcnma1, Kif5c, Krt75, Krt80, Lpcat1, Lyplal1, Lysmd3, Med12l, membrane metallo endopeptidase, Myh14, Ndrg1, Ndrg2, Ndrg4, Nfil3, Nptx1, Nrbf2, Nt5dc2, Nudt4, Nudt11, Palld, Pawr, Pcbd1, Pcbp3, Pdlim3, Pdzk1ip1, Pdzm3, Peg3, Phyhipl, Pkp2, Pmp22, Pole4, Ppargc1a, Ppm1m, Pptc7, Ppp1r3c, Ppp2r1b, Pptc7, Prkcm, Prmt2, Pter, Ptpla, Pvt1, Rabep1, Rai14, Rhou, Rnf208, Scara3, Selenbp1, Serpinb11, SH3 domain containing ring finger1, Slc39a8, Slc6a6, Speg, Spg20, Spsb2, Sqrdl, St8sia2, Stbd1, Stx6, Syt9, Tacc2, Tbc1d19, Tekt2, Tmcc2, Tns1, Tor3a, Trim2, Trpv4, Ttpa, Tubb2a, Tubb2b, Tuft1, Wwp2, Zfp185		

Down-regulated gene after BMP inhibition

Up-regulated gene after BMP inhibition

Fig. S6. Common hfSC and HG signature genes affected by BMP signaling—a BMP master "switch." More than 50% of all down-regulated signature genes in the HG (18 of 35 genes) were affected by BMP inhibition. Strikingly, all of these BMP-dependent HG down-regulated signature genes were found in the signature of the quiescent bulge, although up-regulated. Thus, BMP signaling works as a main "switch" to activate quiescent hfSCs in a very defined and synchronized manner, leading these cells to partially adopt an intermediate active stage resembling the HG with stem cell properties that we tentatively name stem cell/hair germ status.

Table S1. BMP affects commonly up-regulated hfSC signature genes

Table S1

Microarray dataset reveals down-regulation of 103 probes (green type) of 426 probes of commonly up-regulated hfSCs signature genes after inhibition of BMP signaling in hfSCs whereas 16 probes were up-regulated (red type).

Table S2. Hair-germ signature genes affected by BMP signaling

Table S2

Microarray dataset demonstrates that cKO^{RU} hfSCs acquire some molecular characteristics resembling the HG; 32% of the previously characterized HG signature genes (26 genes of 81) were either up- or down-regulated following BMP inhibition (genes in red and green type, respectively). Surprisingly, only three genes characterized in cKO^{RU} hfSCs did not follow similar changes observed in the HG signature genes. In fact, BMP6, NFATc1, and Col20α1 were inversely regulated.